An Electrophoretic Study of Reversible Protein Denaturation: Chymotrypsinogen at High Pressures†

S. A. Hawley* and R. M. Mitchell‡

ABSTRACT: When reversible denaturation of chymotrypsinogen is produced at elevated hydrostatic pressures, conformational relaxation can occur quite slowly, allowing electrophoretic separation of the principal states from the equilibrium mixture. In this work we report experimental concentration distribution patterns obtained at pH 2.03 at a temperature of 20.5° and find them to be reasonably consistent with the behavior that is expected from a simple two-state isomerism. However, the results do not at all rule out the existence of low levels of intermediate states.

It is a characteristic of many experiments involving the reversible denaturation of small globular proteins that the thermochemical properties are dominated by the relative abundance of the native and denatured species. In recent years, however, there have been a number of important investigations of the dynamic evolution of these transitions (recently reviewed by Baldwin, 1975) which have successfully demonstrated the presence, albeit not the detailed character, of the intermediate states. By use of rapid perturbation techniques, particularly those involving pH and temperature-jump, it has been found that the temporal evolution of the conformational features in most cases departs from the single exponential decay which one most simply associates with a two-state isomerism. Thus, reversible denaturation of small globular proteins is perhaps best described as a "three-state process" involving, in addition to the native and denatured states, a "transformational state" corresponding to a set or perhaps even a sequence of partially folded intermediates.

In this investigation we are principally concerned with the electrophoretic separation of the two principal conformations that are associated with pressure denaturation of chymotrypsinogen A. Of particular interest is the comparison of electrophoretic behavior with data obtained from uv absorbance measurements under more conventional, i.e., spatially uniform, conditions. The two-state model plays an important role here in the sense that it provides a satisfactory basis by which all the results may be compared. The question of intermediate states appears only indirectly. For reasons of theoretical convenience, the transformation of each molecule is assumed to occur as an instantaneous event with the consequence of excluding molecules in intermediate states entirely from the equilibrium population. Although the electrophoretic behavior graphically demonstrates the general utility of this approximation, little additional information about the transformation state is provided due to inherent uncertainties in the experimental results.

Experimental Section

At the outset of the investigation, a 6-l. supply of 0.01 *N* HCl (pH 2.03, 20°) was prepared and subsequently employed as solution buffer and final rinse agent for glassware as well as the reservoir buffer for all electrophoresis runs. Chymotrypsinogen A was obtained as a salt-free, crystalline preparation from Schwarz/Mann Laboratories, Freehold, N.J. A stock solution with a protein concentration of 2 mg/ml was prepared and used directly for electrophoresis and diluted to 0.9 mg/ml for ultraviolet absorbance measurements.

Separate, but quite similar, pressure systems were employed for absorbance and electrophoresis experiments. Both were simple hand-pump, piston-intensifier arrangements (Bridgman, 1931). Pressure was measured (±20 kg cm^{-2}) by determining the change of resistance of a manganin coil immersed in the intensifier cylinder.

Absorbance Measurements. The physical arrangement, including the sample cell and the technique used to measure the absorbance at 292 nm as a function of pressure, is quite similar to that described previously for equilibrium measurements of chymotrypsinogen (Hawley, 1971; see also Hawley and Macleod, 1974). However, special precautions were necessary prior to the acquisition of kinetic data because the long relaxation times involved in the transition process required that the spectrophotometer, temperature bath, and pressure system be operating continuously over a period of time in excess of 2 weeks. In particular, the double-beam spectrophotometer (Perkin Elmer Model 350) was carefully adjusted for maximum stability, just prior to the investigation. A Pyrex filter was employed in the reference compartment and the instrument was balanced with the optical pressure vessel in the sample compartment so as to minimize the effect of light source aging on the observed optical density.

Usually we refer to the perturbation process as a "pressure" jump. It is more accurate, however, to say that the causative agent is a rapid change in the overall internal volume of the pressure system which is produced by movement of the piston in the intensifier cylinder. If this could be done very quickly, the trajectory of the pressure and temperature would be more nearly adiabatic than isothermal with the relaxation to equilibrium pressure and temperature determined by a number of physical constraints present in the system. Potentially the slowest process of concern is the relaxation of temperature gradients that arise. These can be quite large. Based on the thermodynamic properties of water, we estimate that the adiabatic heating or cooling

† From the Jefferson Physical Laboratories, Harvard University, Cambridge, Massachusetts 02138. *Received March 13, 1975.* This work was supported by grants from the National Institutes of Health and the National Science Foundation.

‡ Present address: Department of Physics, Wellesley College, Wellesley, Massachusetts.

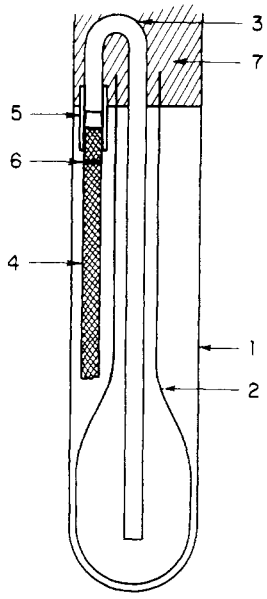

FIGURE 1: Electrophoresis cell for high pressure experiments. Pyrex test tube (1) serves as a container for the cell assembly. The inner reservoir compartment (2) contains the anodal buffer for chymotrypsinogen experiments. The glass tube (3) contains a buffer providing a conductive bridge to the gel tube (4); the two are joined by a short segment of latex tubing (5). Initial location of the protein solution (6). Platinum electrodes (not shown) are inserted from above through the hydraulic fluid (7), which in these experiments is petroleum ether.

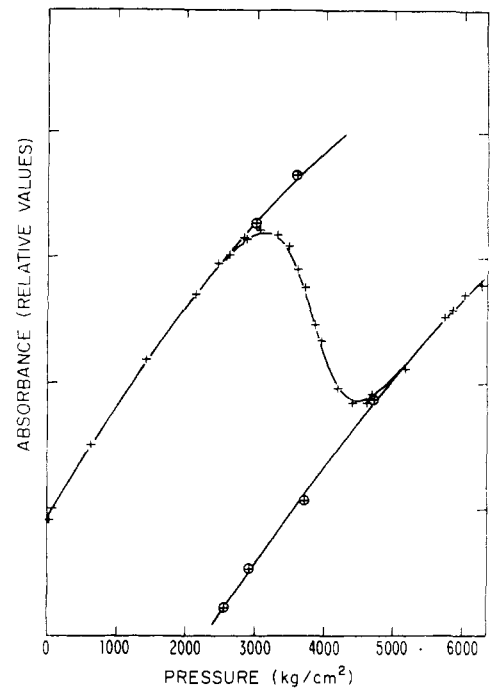

FIGURE 2: Relative absorbance vs. pressure at 292 nm, 20.5°. Circled points show the absorbance immediately following a pressure jump from the base-line region; the remaining points represent equilibrium data. The solid line through the transition points represents the calculated absorbance data using a van't Hoff (two-state) thermodynamic analysis.

amounts to 2.5° per 1000 kg cm^{-2}. To minimize this effect, the sample holder (Hawley and Macleod, 1974) was constructed of a very thin (5 mil) Teflon cylinder which is surrounded by a ring having a high thermal diffusivity. The characteristic time associated with the decay of the adiabatic heat is estimated at about 10 sec. Although we will be presenting results of pressure-jump experiments which in some instances required displacements in excess of 3000 kg cm^{-2}, in all cases the macromolecular relaxation of the absorbance is at least ten times slower than that attributable to other sources.

The temperature of the sample was maintained at 20.5° by circulating a mixture of ethylene glycol and water through a jacket surrounding the exterior of the pressure vessel. A quartz thermometer probe was employed to monitor the temperature of the pressure vessel; during these experiments the temperature was observed to drift slowly producing an overall uncertainty of about ±0.2°.

Gel Electrophoresis. Polyacrylamide gels with 10% acrylamide, 0.3% methylbisacrylamide cross-linking agent, and no buffer were formed as 5.5-cm columns in 3.8-mm i.d. Pyrex glass tubes. Prior to use, these tubes were boiled in chromic acid, thoroughly rinsed, and oven dried. Gel columns were poured in batches of about 30 until a suitable set of gels was obtained in a single batch. Because the investigation demands that the gel columns be relatively uniform in their properties, entire batches were rejected if there appeared any evidence to the contrary.

Once formed, the gels were carefully rinsed with water and subsequently allowed to soak in buffer for 1 week to allow penetration of ions into the gel network. Next the gels were prerun for 3 hr in both directions at a current of 2 mA/gel. After prerunning a 1-cm segment was snapped off the bottom end, providing a set of gel plugs which were eventually used to trap the protein solution on the gel meniscus. All gel columns were then allowed to soak for about 1 month with a weekly change of buffer to ensure dissipation of any pH gradients that occurred in the prerunning process.

The electrophoresis apparatus was a relatively simple extension of standard electrophoretic techniques to accommodate the demands imposed by elevated hydrostatic pressure—which is primarily one of limited working volume. In this investigation the entire electrophoresis cell was contained in a single 30-ml Pyrex test tube (Figure 1). A second tube, blown into the shape of a small volumetric flask, was inserted in order to partition the volume into two reservoirs. The gel column forms part of a bridge between the two buffer compartments, hanging in the annular space formed between the reservoirs. Electrical connections were made via platinum electrodes inserted from above into the reservoir compartments. The pressure vessel was a simple tool steel block which was mounted in a 50-gal thermostatic bath.

For all electrophoresis runs, the gels were charged by placing 12 μl of the stock solution on the gel meniscus. A 5-mm gel plug was inserted into the end of the tube. It was not necessary to push this plug manually against the meniscus since this occurs automatically when pressure is applied.

The cell assembly is inserted in the pressure vessel and incubated for 24 hr at the desired pressure and temperature prior to running. Runs were made with a current of 1.96 mA for 7200 sec. The use of a constant current source was a practical convenience; during the run the applied voltage was continuously monitored and recorded.

Immediately following electrophoresis the gel was removed by gently crushing the glass tube, and was then scanned at 280 nm. The ultraviolet scans, while useful, were usually marred by the presence of small optical imperfections on the surface of the gel column, presumably created in the process of releasing it from the glass tube. The gels were then stained with Coomassie Brillant Blue, destained

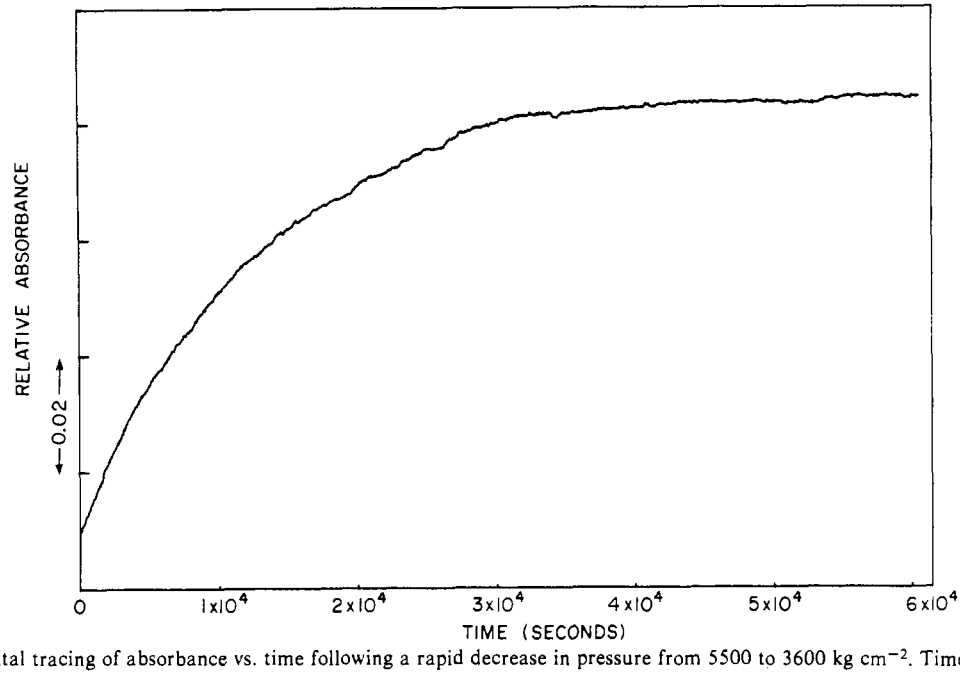

FIGURE 3: Experimental tracing of absorbance vs. time following a rapid decrease in pressure from 5500 to 3600 kg cm^{-2}. Time constant is about 12,500 sec.

in a methanol–water mixture, and subsequently scanned at 625 nm. The signal-to-noise ratio was substantially better for the stained gels. Analysis of the correlation between the ultraviolet and visible scans indicated that within experimental error the absorbance in excess of background at 280 nm was in good accord with that at 625 nm at any point, and so only the latter results will be presented here.

In order to estimate the diffusion coefficient of the protein in the gel matrix, two series of free-diffusion experiments were conducted, one at atmospheric pressure and one at 5000 kg cm^{-2}. Here gel tubes were suspended in the protein solution and incubated for periods of up to 15 days. The gels were subsequently stained and scanned as in the electrophoretic runs. Because the boundary conditions are fairly complex in these experiments, the estimated uncertainty in the diffusion coefficients calculated from these experiments is of the order of 20%.

Results

Absorbance Measurements. Two well-determined absorbance base lines are observed above and below the transition (Figure 2). In order to evaluate the equilibrium constant, K, as a function of pressure it is necessary to determine the pure state absorbance properties, α_N and α_D, throughout the range of reaction. When the transition velocity is relatively rapid—as is often the case for thermal denaturation at ambient pressures—it is necessary to determine α_N and α_D by extrapolating values of the absorbance from the respective base lines. In the pressure denaturation of chymotrypsinogen, and as we have generally found to be the case for pressure denaturation of other proteins, the relaxation of conformational features occurs so slowly that it is usually difficult to locate the onset of denaturation in the first passage through the transition. The absorbance, instead, continues along a trajectory consistent with extrapolation of the base line until a situation is reached in which the total elapsed time that the system has been in a nonequilibrium state is sufficiently great to indicate the presence of the molecular transition. Thus, when the pressure is jumped deliberately from either base line into the transition region it is relatively simple to observe a metastable behavior in which the external variables, pressure and temperature, have equilibrated but the internal variables associated with the molecular state have changed very little. This behavior permits direct measurement of α_N and α_D within the transition region and, further, reduces the degree to which extrapolation is necessary in thermodynamic analysis. The optical properties of these "metastable" states are, of course, not perfect since the reaction rate, while small, is not zero. In these experiments, however, it was a relatively simple matter to extend the native base line to above the transition midpoint and the denatured base line completely through the transition without the occurrence of significant amounts of reaction. The resulting "metastable" absorbance values are indicated as open circles in Figure 2. The total pressure dependence of α_N and α_D was established in each case by including these additional points.

Although the metastable behavior by itself implies the absence of a rapid initial decay process, such as that seen in temperature-jump experiments (Tsong and Baldwin, 1972), we were somewhat surprised to find that for all perturbation experiments, even those employing large pressure increments, the relaxation of the absorbance followed a simple single exponential decay such as that shown in Figure 3. The strict adherence to first-order kinetics is not a general feature of our work with other proteins. For both ribonuclease and staphylococcal nuclease, a small (5%) rapid change has been observed in pressure-jump experiments under circumstances in which the final equilibrium state was in either native or denatured base-line region. Chymotrypsinogen thus represents a particularly interesting case in the sense that it completely fulfills the kinetic requirement generally set out as a criterion for a two-state transformation (i.e., it must be a first-order process; Baldwin, 1975). Since we do not believe the presence of intermediates is ruled out by these experiments, the situation is illustrative of a possible weakness in this kinetic rule. It would seem appropriate to say only that the population of intermediate states is never appreciable in the pressure experiments. Because the relaxation process is, overall, so slow the lifetime associated

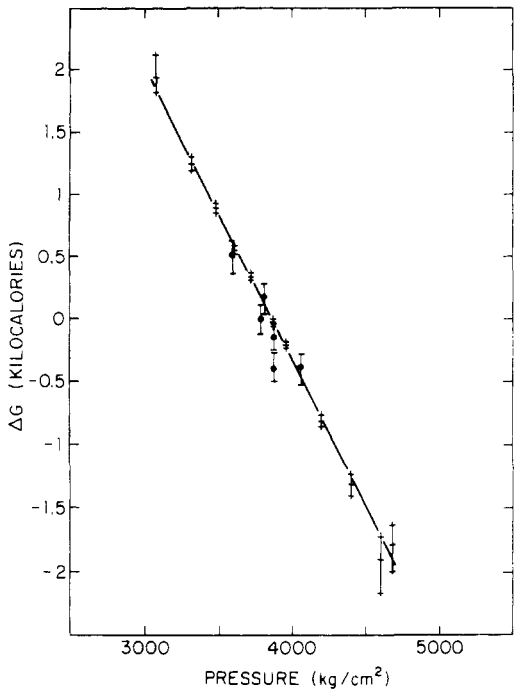

FIGURE 4: Apparent free energy vs. pressure for chymotrypsinogen at 20.5°. The filled circles represent electrophoretic data, the remainder represent absorbance behavior. The least-squares value for the slope of the absorbance data is -94 cm^3/mol—that is, the thermodynamic volume of the denatured state is *smaller* than that of the native state.

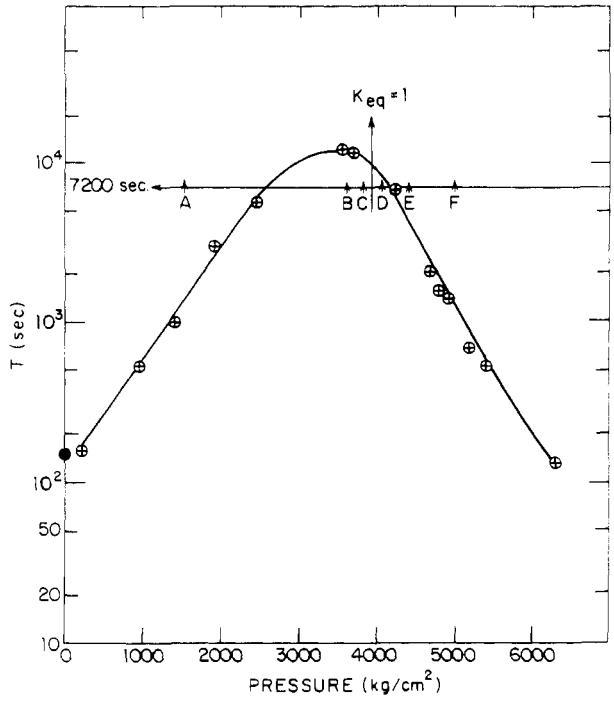

FIGURE 5: Relaxation data for absorbance measurements showing the effect of pressure on the characteristic time, τ. The apparent transition midpoint ($K_{eq} = 1$) is indicated as well as the location of the electrophoretic experiments shown in Figure 8. Filled point at ambient pressure was taken from the temperature-jump data of Pohl (1969) for chymotrypsinogen A at pH 2.

with the intermediate states could be as long as several seconds and still account for less than 1% of the total equilibrium population.

The process of embedding the equilibrium experimental information into a two-state thermodynamic model must be done with the realization that it is not exact but rather a very good approximation; the distinction is important since ultimately it is the intermediates which are of greatest interest. The "embedding" procedure is well-known, and for isothermal pressure denaturation it provides a phenomenological relation between the relative population of the principal states and the applied pressure, via the transition volume increment ΔV. Having determined the pressure dependence $\alpha_N(P)$ and $\alpha_D(P)$ of the absorbance in the native and denatured states, one has

$$\alpha(P) = X_N\alpha_N + X_D\alpha_D$$
$$1 = X_N + X_D$$

Consequently

$$K = X_D/X_N = (\alpha_N - \alpha)/(\alpha - \alpha_D)$$

The free energy difference is calculated from the relation $G_0 - G_N = \Delta G = -RT \ln K$. To first-order terms in pressure we write $\Delta G = \Delta G_0(P,T) + \Delta V(P - P_0)$, so that the volume increment, $\Delta V = -RT(\partial \ln K/\partial P)_T$ is determined from a linear regression of the pressure dependence of the apparent free-energy difference ΔG.

In the present experiments the relation was found to be reasonably linear (Figure 4); the presence of higher order terms, particularly that due to the compressibility, is not as evident as it is in studies of stability in which a wider range of pressures and temperatures is examined (Hawley, 1971; Brandts et al., 1970). A least-squares regression of the absorbance data which appear in Figure 4 indicates $\Delta G_0 = 9000$ cal mol^{-1} and $\Delta V = -94$ cm^3 mol^{-1}. Both values are in reasonable agreement with previous results from this laboratory for which ΔV was estimated to be -110 cm^3 mol^{-1} (Hawley, 1971). This information, in conjunction with experimentally determined values for $\alpha_N(P)$ and $\alpha_D(P)$, allows us to work backwards to reconstruct the total absorbance $\alpha(P)$, which is shown in Figure 2 as the solid line through the transition points.

The time-dependent absorbance was fit to a single exponential decay, $\delta\alpha(t) = \delta\alpha_0 e^{-t/\tau}$, resulting in χ^2 behavior consistent with this functional form within the limitations of experimental error. The pressure dependence of τ (Figure 5) is qualitatively similar to that found for staphylococcal nuclease and ribonuclease, all exhibiting a maximum value within the transition region.

Electrophoretic Results. The electrophoretic behavior of the unimolecular isomerization process, N $\rightleftharpoons$ D, has been examined theoretically on several occasions (Cann and Bailey, 1961; Scholten, 1961; Van Holde, 1962). An important element of these discussions is that the theoretical model which is employed to develop the transport properties assumes the two-state hypothesis so often associated with considerations of reversible protein denaturation. That is, the system is assumed to contain a molecular species which is capable of exhibiting either of two hydrodynamic states; each state having its own characteristic mobility and diffusion coefficient. If k_1 is the probability per unit time to switch from state N to state D and k_2 the probability per unit time to switch from state D to state N, then in the absence of an external field relaxation behavior is described by the familiar master equations, viz.

$$d\delta X_N/dt = -k_1X_N + k_2X_D$$
$$d\delta X_D/dt = k_1X_N - k_2X_D$$

These equations require the transition kinetics to follow a

single exponential course under all conditions with a relaxation time $\tau = (k_1 + k_2)^{-1}$.

The most interesting behavior, of course, occurs when the concentration distribution pattern in the gel displays two well-resolved peaks corresponding to the principal conformational states. The fact that the pressure transition of chymotrypsinogen provides such behavior was established in a preliminary report (Hawley, 1973). We have also observed similar although considerably less dramatic behavior in the pressure transitions of ribonuclease (pH 2.5) and myoglobin (pH 4.5) at subzero Celsius temperatures. At these temperatures with chymotrypsinogen, the transition occurs so slowly that evidence of separate electrophoretic peaks persisted even in experiments which lasted as long as 72 hr.

In probing the electrophoretic properties, perhaps the most useful gauge of the possibility of producing peak separation is derived from the determination of the pure state mobilities as a function of the perturbing external parameter, in this case, the hydrostatic pressure (Figure 6). Extrapolation of mobilities of the principal states from the base lines into the transition region provides the measure of the maximum separation that can be achieved in the transition region in a given time. The extent to which such separation can actually be produced will be determined by one's ability to conduct the electrophoresis run over a sufficiently small fraction of the relaxation time.

The electrophoretic run-time which is finally chosen, however, must be sufficiently long to produce peak separation which is greater than the initial width of the protein layer. With an initial solution thickness of 1.3 mm and field-free diffusion coefficients $D_N = 1 \times 10^{-7}$ cm^2 sec^{-1} and $D_D = 0.8 \times 10^{-7}$ cm^2 sec^{-1}, we estimate that after the 24-hr incubation period which is required to bring the system to equilibrium, the characteristic electrophoretic zones will have spread to widths of about 2.8 and 2.7 mm for the respective states. The total observed width for each peak is at least twice this, varying between 5 and 7 mm (left-hand panels, Figure 7). We do not know the origin of the additional diffusive process, which appears for both pure and transional states. It occurs independent of incubation time, and we suspect that it arises in part as the result of mass-flow processes which occur during initial pressure application and in part may be attributable to nonlinear transport during the early stages of electrophoresis. It is clear, however, that the additional width is not the result of the molecular transition. The principal effect resulting from its presence was the imposition of a longer run-time in order to produce favorable resolution. To show the relationship of the run-time to the kinetic properties of the transition we have inserted the value employed (7200 sec) as a separate axis in Figure 5 on which is indicated the location of experiments for which the concentration patterns shown in Figure 7 were produced. It is evident that at this temperature (20.5°) the pressure dependence of the relaxation time is such that kinetic conditions most favorable for separation occur in the transition region where the relaxation curve passes above the inserted run-time axis.

For comparison the right-hand panels of Figure 7 show calculated concentration distributions corresponding to the experiment shown in the adjacent left-hand panel. The method of calculation did not follow either of the usual procedures, which involve numerical evaluation of the transport equations (Cann and Bailey, 1965) or their Fourier transforms (Scholten, 1961). Rather, it is based on an exact, closed solution of these equations which is briefly discussed in the Appendix. The theoretical curves do not represent an attempt to fit the experimental data exactly but rather develop from the simplest initial conditions that would be reasonably consistent with this system. Specifically, it has been assumed for purposes of calculation that at $t = 0$ the protein solution begins its traversal from an infinitesimal laminum at equilibrium on the end of the gel. The measured field-free diffusion coefficients have been used although the diffusion process in the presence of an electric field may be slightly different due to charge fluctuation effects. The theoretical patterns, therefore, represent the kind of patterns one might hope to obtain under more ideal experimental circumstances.

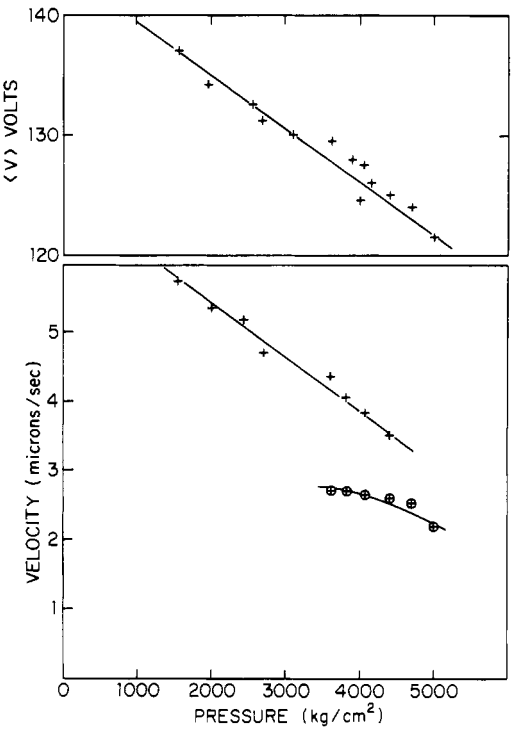

FIGURE 6: (Upper panel) Average voltage (at constant current) for 2-hr electrophoretic run-time at various pressures. Values were obtained by integrating the instantaneous voltage over the run-time and dividing by 7200. (Lower panel) Apparent electrophoretic mobility vs. pressure. Crosses correspond to native state, circles to the reversibly denatured state.

They usefully show, however, that the spread in the distribution that arises in conjunction with molecular switching is relatively minor near the transition midpoint (panels h, i, and j) forming mainly a low level background and causing little loss in resolution. For run-times T less than the relaxation time τ the areas under the respective peaks should provide a rough measure of the equilibrium constant. To test this we have determined an apparent equilibrium constant, equal to the ratio of peak areas for these and other experiments, and find the corresponding free energy in reasonable agreement with the absorbance data (Figure 6).

As is the case for other proteins such as ribonuclease (Brandts et al., 1970) and myoglobin (Zipp and Kauzmann, 1973) the apparent volume decrease associated with pressure denaturation of chymotrypsinogen is small and cannot be reconciled in a simple way with models of hydrophobic bonding. Because the van't Hoff thermodynamic behavior estimated from electrophoretic evidence is consistent with this absorbance data no additional insight into this matter is provided from the population distributions.

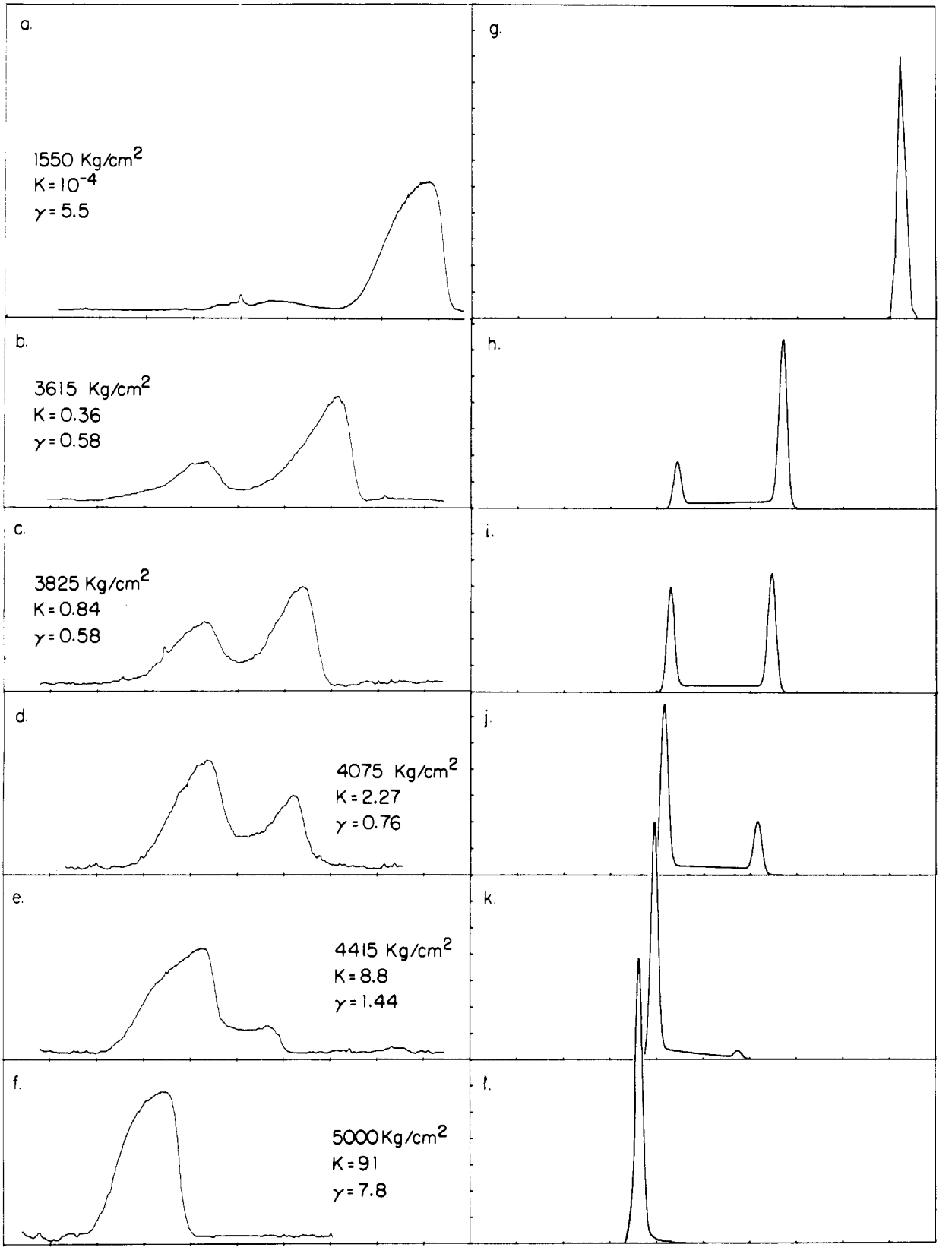

FIGURE 7: (Left-hand panels (a–f)) Experimental concentration distributions at six pressures. The equilibrium constant K is X_D/X_N, and the ratio of electrophoretic run-time to the observed relaxation time, $\gamma = T/\tau$, is listed for each run. Here $\tau = (k_1 + k_2)^{-1}$. The experimental peaks are broader than the theoretical because not all the protein enters the gel at the same time. (Right-hand panels (g–l)) Theoretical concentration distributions corresponding to adjacent experiments. The right-hand panels are drawn assuming that all the protein enters the gel at the same time, and that the boundaries can be ignored. Further details of the theoretical distribution function can be found in the Appendix. Each panel corresponds to a length of 4.5 cm and abscissas are marked in one-tenth parts; electrophoresis begins at the left of each panel and proceeds as the molecules move to the right. Both experimental and theoretical curves have been normalized to constant area. The normalized area for the experimental curves, however, is about five times larger than for the theoretical distributions.

Discussion

In some respects the results, although clearly limited in scope, are reassuring. They indicate that the two-state representation provides a relatively self-consistent model that extends beyond equilibrium situations. This, however, does not tell us very much about the intermediate states; their presence is sustained here, thus far, primarily as a logical necessity. In the pressure denaturation experiments it seems quite clear that each molecule spends virtually all its time as either of two distinct species and relatively little time making the transformation. Evidently the thermodynamic character of the intermediate states is quite unfavorable. This may only mean that the transformation process represents a narrowly defined sequence of molecular states, so that the number of configurations involved is a very small fraction of the *total* variants available to the protein. In this situation, each molecule would spend most of its existence sorting through the numerous molecular forms associated with either the native or denatured species until it found itself in an intermediate state and thereby able to make a transformation. The situation is akin to that of partitioning a suspension of small, nontransforming particles into two populations by a membrane which is permeable to both the particles and suspending fluid; instead of two states, we have the two volumes on either side of the membrane. An equilibrium constant can be defined as the ratio of the numbers of particles on either side. While this would provide an adequate description for many purposes the transitional states—those with particles in the membrane passageways—are neglected, as in the two-state model. If the volume of suspension on either side of the membrane is much greater than that contained within it, the dynamical behavior associated with population redistributions following a perturbation would be affected only indirectly by the details of the membrane pores. The rate-limiting step is not the time that occurs in passage through the membrane but rather the much greater time spent by each particle in random flight before finding a pore.

In the case of protein denaturation, of course, the random flight is in configuration space as opposed to physical space. The existence of a large configurational space is most readily seen for the denatured protein which is often characterized as a random coil, thus implying directly the existence of a large population of more or less equally likely configurations of the polypeptide backbone. The native state would appear to be less amenable to the idea of such a population. However, the configurational space almost surely extends to include at least a portion of the aqueous surroundings. The necessity of this can be seen in the pressure denaturation phenomena. In our experiments, the isotherm which was utilized crosses the coexistence lines for the transition in a region where they are nearly temperature independent (cf. Hawley, 1971); this requires that the entropy difference associated with denaturation be very small. Thus, there must be some ordering process, presumably in the solvent, which compensates for the randomization of the backbone. Although the pressure-denaturation data do not allow us to specify the molecular details of the compensating process, they assure us of its presence. A simple interpretation of the longevity of the native state in the transition mixture, then, is just that each molecule is required to sort through many possible configurations in the surrounding solvent structure before encountering one which accommodates the transformation process.

Appendix

We wish to find the density distribution of particles which change from state A to state B with probability k_1 per unit time and from state B to state A with probability k_2 per unit time. All particles start ($t = 0$) at $z = 0$. While they are in state A, particles move at speed v_A in the applied electric field and diffuse with diffusion coefficient D_A, and similarly in state B. The density distribution $\rho_{TOT}(z,t)$ of all particles at time t is calculated in two parts

$$\rho_{TOT}(z,t) = X_A\rho(z,t) + X_B\tilde{\rho}(z,t) \qquad \text{(A1)}$$

where ρ and $\tilde{\rho}$ are normalized probability distributions referring to particles which began in state A and state B, respectively. Here X_A is the fraction of particles which began in state A and $X_B = 1 - X_A$ is the fraction which began in state B. If the molecules have been allowed to come to chemical equilibrium before turning on the electric field, then we have

$$X_B/X_A = k_1/k_2 = K \qquad \text{(A2)}$$

where K is the equilibrium constant at the given temperature, pressure, and pH. We find $X_B = K/(K + 1)$, $X_A = 1/(K + 1)$.

The explicit evaluation of the distribution $\rho(z,t)$ for molecules beginning in state A (or state B) can be performed by direct probabilistic reasoning (Mitchell, 1975); the result is much more appealing on physical grounds (and also much more convenient for computer analysis) than the standard treatment employing master equations (Scholten, 1961), which expresses the answer in the form of a Fourier integral. We evaluate the contribution to $\rho(z,t)$ from molecules which have switched states 0,1,2,3, . . . ,∞ times. It is found that all of the terms corresponding to an even number of switches (i.e., the molecules wind up in the original state, A) are of the same form, and likewise for the terms arising from an odd number of switches. The net result for $\rho(z,t)$ can be written

$$\begin{aligned}\rho(z,t) = \rho_0(z,t) + \rho_{odd}(z,t) + \rho_{even}(z,t) = \\ \frac{1}{\sqrt{4\pi D_A t}}\exp\{-(z - v_A t)^2/4D_A t\}e^{-k_1 t} + \\ k_1 e^{-k_2 t}\int_0^t dT\left(\sum_{m=0}^{\infty}\frac{\{k_1 k_2 T(t - T)\}^m}{(m!)^2}\right)\times \\ \frac{e^{(k_2-k_1)T}\exp\left(-\frac{\{(v_B - v_A)T + z - v_B t\}^2}{2\sigma_1^2(T)}\right)}{\sqrt{2\pi\sigma_1^2(T)}} + \\ e^{-k_1 t}\int_0^t dT\left(\sum_{m=1}^{\infty}\frac{\{k_1 k_2 T(t - T)\}^m}{Tm!(m - 1)!}\right)\times \\ \frac{e^{(k_1-k_2)T}\exp\left(-\frac{\{(v_A - v_B)T + z - v_A t\}^2}{2\pi\sigma_2^2(T)}\right)}{\sqrt{2\pi\sigma_2^2(T)}}\end{aligned} \qquad \text{(A3)}$$

with $\sigma_1^2 = 2(D_A - D_B)T + 2D_B t$, $\sigma_2^2 = 2(D_B - D_A)T + 2D_A t$, where the first term corresponds to molecules which have not switched at all, the second term corresponds to molecules which have switched 1,3,5, . . . , ∞ times, and the third to molecules which have switched 2,4,6, . . ., ∞ times. Similarly, the fraction, X_B, of molecules beginning in state B will have a spatial distribution $\tilde{\rho}(z,t)$ which has exactly the same form as $\rho(z,t)$, but with subscripts A and B, 1 and 2 interchanged.

The total distribution $\rho_{TOT}(z,t)$ is then the weighted sum (A1) of $\rho(z,t)$ and $\tilde{\rho}(z,t)$. For purposes of evaluation by

computer, it is convenient to introduce (Cann and Oates, 1965) the dimensionless variable $t_0 = t/\tau_A$ and $z_0 = z(D_A\tau_A)^{-1/2}$, where $\tau_A = 1/k_1$, and to view the electrophoresis from a frame of reference moving at the average speed $\bar{v} = \frac{1}{2}(v_A + v_B)$, also let $D_B = rD_A$. The distributions $\rho(z_0,t_0)$ and $\tilde{\rho}(z_0,t_0)$ are then obtained from $\rho(z,t)$ and $\tilde{\rho}(z,t)$ by replacing k_1 with 1, k_2 with K^{-1}, v_A with $-\beta/2$, v_B with $+\beta/2$, D_A with 1, D_B with r, and, of course, z with z_0 as well as t with t_0. The right half of Figure 7 was computed using this procedure; because the integrand in (A3) is nonoscillatory and the limits of integration are finite (t_0 is typically on the order of unity), the integral requires very little computer time for each value of z.

For the special case of irreversible isomerization, A → B, the distribution ρ is extremely simple (there is no distribution $\tilde{\rho}$ needed):

$$\rho(x,t) = \frac{1}{\sqrt{4\pi D_A t}} \exp\left\{-\frac{(x - v_A t)^2}{4D_A t}\right\} e^{-kt} + k \times \int_0^t \frac{\exp(-\{x - v_B t + (v_B - v_A)t_1\}^2/\{4(D_A - D_B)t + 4D_B t\})}{\sqrt{4\pi\{(D_A - D_B)t_1 + D_B t\}}} \times e^{-kt_1} dt_1$$

It should be noted also that the formalism, for both reversible and irreversible cases, can be applied to a bimolecular reaction, such as binding of a ligand by a macromolecule, if the ligand is present in sufficient excess so that the reaction rate is essentially constant.

For the calculations that appear in Figure 7 we have used the following properties of the native state, $v_A = 7 - 7.7 \times 10^{-4P}$ cm sec^{-1} (P in kg cm^{-2}), $D_A = 1 \times 10^{-7}$ cm sec^{-2}; for the denatured state, $v_B = 4.07 - 3.6 \times 10^{-4}P$, $D_B = 0.8 \times 10^{-7}$ cm sec^{-2}. Values of $\tau = (k_1 + k_2)^{-1}$ were obtained from interpolation of data shown in Figure 5 and $K = k_2/k_1$ was obtained from the relation $K(P) = \exp\{-(9013 - 2.33P)/RT\}$ with P again measured in kg cm^{-1}.

It is worth mentioning, as an afterthought to the experimental stages of this work, that electrophoretic analysis can provide a useful source of thermodynamic information even when physical separation of states is not possible. In fact, for the two-state process when the relaxation time is very short compared to the run-time, the fraction of time spent in each state during transit will approach its equilibrium population fraction. The entire population will move as a single band with a mean speed $\bar{v}$ given by

$$\bar{v} = X_A v_A + X_B v_B$$

where X_A and X_B are the fraction of molecules in the respective states. The measured band velocity, then, will behave in the same way as more familiar observable properties such as absorbance or optical rotation. In order to determine the dependence of the equilibrium constant on an external parameter ξ such as pressure or temperature it is necessary to determine $\bar{v}(\xi)$ over the full range of the transition plus portions of the respective base-line regions. The equilibrium constant is then

$$K(\xi) = \{v_A - \bar{v}(\xi)\}/\{\bar{v}(\xi) - v_B\}$$

Extrapolation is, of course, necessary to provide values of v_A and v_B in the transition region. The nature of the external variable is not restricted to pressure and temperature and may include chemical composition as long as it remains uniform over the spatial extent of the reaction and does not involve concentrations which are substantially depleted by interactions with the protein.

Thus, whether or not physical separation of conformational states is possible, electrophoresis can always be considered as a potential analytical tool for conformational transition processes.

References

Baldwin, R. L. (1975), *Annu. Rev. Biochem.* (in press).

Brandts, J. F., Oliverira, R. J., and Westort, C. (1970), *Biochemistry 9,* 1038.

Bridgman, P. W. (1931), The Physics of High Pressures, London, Bell and Sons.

Cann, J. R., and Bailey, H. R. (1961), *Arch. Biochem. Biophys. 93,* 576.

Cann, J. R., and Oates, D. C. (1973), *Biochemistry 12,* 1112.

Hawley, S. A. (1971), *Biochemistry 10,* 2436.

Hawley, S. A. (1973), *Biochim. Biophys. Acta. 317,* 236.

Hawley, S. A., and Macleod, R. M. (1974), *Biopolymers 13,* 1417.

Mitchell, R. M. (1975), Ph.D. Thesis, Physics Department, Harvard University, Cambridge, Mass.

Pohl, F. M. (1969), *FEBS Lett. 3,* 60.

Scholten, P. C. (1961), *Arch. Biochem. Bioplys. 93,* 576.

Tsong, T. Y., and Baldwin, R. L. (1972), *J. Mol. Biol. 69,* 1972.

Van Holde, K. E. (1962), *J. Chem. Phys. 37,* 1922.

Zipp, A., and Kauzmann, W. (1973), *Biochemistry 12,* 4217.